BRAIN COMMUNICATIONS

Role of glucosamine in development of diabetic neuropathy independent of the aldose reductase pathway

Hiroki Mizukami,[1] Sho Osonoi,[1] Shizuka Takaku,[2] Shin-Ichiro Yamagishi,[1] Saori Ogasawara,[1] Kazunori Sango,[2] Sookja Chung[3] and Soroku Yagihashi[1]

Long-term metabolic aberrations contribute to the development of diabetic neuropathy but the precise mechanism or mechanisms remains elusive. We have previously shown that aldose reductase-deficient mice exhibit delayed onset and progression of neuropathy following induction of diabetes, suggesting a role both for downstream metabolites of this enzyme and also for other unrelated pathways. In this study, we have utilized comprehensive metabolomics analyses to identify potential neurotoxic metabolites in nerve of diabetic mice and explored the mechanism of peripheral nerve injury. Aldose reductase knockout and control C57Bl/6J mice were made diabetic by injection of streptozotocin and followed for 8–16 weeks. Diabetic aldose reductase knockout mice exhibited delayed onset of nerve conduction slowing compared to diabetic wild-type mice. The sciatic nerves from aldose reductase knockout mice exposed to 12 weeks of diabetes were used for metabolomics analysis and compared with analyses of nerves from age-matched diabetic wild-type mice as well as non-diabetic aldose reductase knockout and wild-type mice. Neurotoxicity of candidate metabolites was evaluated using cultured Schwann cells and dorsal root ganglion neurons, and further confirmed *in vivo*. Metabolomics analysis identified elevated glucosamine levels in both diabetic aldose reductase knockout and diabetic wild mice. Exposure to glucosamine reduced survival of cultured Schwann cells and neurons accompanied by increased expression of cleaved caspase 3, CCAT-enhancer-binding homologous protein and mitochondrial hexokinase-I, along with ATP depletion. These changes were suppressed by siRNA to hexokinase-I or the ATP donor, inosine, but not by the antioxidant N-acetylcysteine or the endoplasmic reticulum-stress inhibitor 4-phenylbutyrate. The O-GlcNAcylation enhancer, O-(2-acetamido-2-deoxy-D-glucopyranosylidene) amino N-phenylcarbamate, did not augment glucosamine neurotoxicity. Single dose glucosamine injection into mice caused a reduction of sciatic nerve Na, K-ATPase activity, ATP content and augmented expression of hexokinase-I, which were suppressed by pretreatment with inosine but not with 4-phenylbutyrate. Mice implanted with a subcutaneous pump to infuse glucosamine for 12 weeks developed nerve conduction slowing and intraepidermal nerve fibre loss, recapitulating prominent indices of diabetic neuropathy. While acute glucosamine neurotoxicity is unlikely to contribute substantially to the slowly developing neuropathy phenotype in humans, sustained energy deprivation induced by glucosamine may well contribute to the pathogenesis of diabetic neuropathy. Our data thus identifies a novel pathway for diabetic neuropathy that may offer a potential new therapeutic target.

1 Department of Pathology and Molecular Medicine, Hirosaki University Graduate School of Medicine, Hirosaki, Japan
2 Diabetic Neuropathy Project, Tokyo Metropolitan Institute of Medical Science, Tokyo
3 Faculty of Medicine, Macau University of Science and Technology, Taipa, Macau

Correspondence to Dr Soroku Yagihashi, Department of Pathology and Molecular Medicine, Hirosaki University Graduate School of Medicine, 5 Zaifu-cho, Hirosaki 036-8562, Japan
E-mail: yagihasi@hirosaki-u.ac.jp

Keywords: diabetic neuropathy; pathogenesis; glucosamine; ATP depletion; metabolome

Received December 13, 2019. Revised August 4, 2020. Accepted August 24, 2020. Advance Access publication October 9, 2020

Abbreviations: AR = aldose reductase; AR-KO = AR-knockout; CC3 = cleaved caspase 3; CHOP = CCAT-enhancer-binding homologous protein; ER = endoplasmic reticulum; F6P = fructose-6-phosphate; GFAT = glutamine-fructose-6-phosphate amidotransferase; GlcN = amino monosaccharide glucosamine; GlcN6P = glucosamine-6-phosphate; HBP = hexosamine biosynthetic pathway; Hex = hexokinase; Hex-I = hexokinase I; MMP = mitochondrial membrane potential; MNCV = motor nerve conduction velocity; O-GlcNAcylation = O-linked addition of N-acetylglucosamine glycosylation; 4PB = 4-phenylbutyrate; PUGNAc = O-(2-acetamido-2-deoxy-d-glucopyranosylidene) amino N-phenylcarbamate; ROS = reactive oxygen species; SNs = sciatic nerves; WT = wild type.

Graphical Abstract

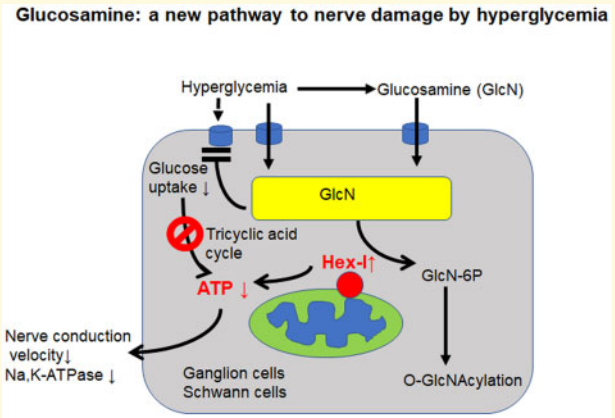

Introduction

Diabetic neuropathy is an early and common complication of diabetes affecting ~35% to 50% of diabetic patients (Vinik *et al.*, 2013; Ziegler *et al.*, 2014). Although long-term hyperglycaemia is likely to be a major culprit that initiates neuropathy, the precise mechanism of how hyperglycaemia leads to neural dysfunction and irreversible nerve fibre damage is yet to be established. Increased polyol pathway mediated by aldose reductase (AR), accumulation of advanced glycation end-products or intermediate glycation products, and increased oxidative stress as well as altered protein kinase C activities are all proposed to be responsible for the development of neuropathy (Oates, 2008; Yagihashi *et al.*, 2011; Vinik *et al.*, 2013; Yagihashi, 2016; Feldman *et al.*, 2017). Despite vigorous efforts to develop an effective compound to prevent or cure diabetic neuropathy, no specific agents have yet been globally approved.

Increased flux through the polyol pathway is one of the most established and extensively studied mechanisms thought to cause diabetic neuropathy (Oates, 2008; Yagihashi *et al.*, 2011; Feldman *et al.*, 2017). Clinical trials of AR inhibitors such as sorbinil or zenarestat disclosed beneficial effects on nerve fibre loss and nerve conduction delay in patients with diabetes (Sima *et al.*, 1988; Greene *et al.*, 1999). Due to serious adverse effects, however, they were withdrawn from the market. Epalrestat, though less potent compared to the above compounds, but free from serious side effects, was found to protect from progressive deterioration of nerve conduction, and to mitigate symptoms of neuropathy in Japanese patients with diabetes (Goto *et al.*, 1995; Hotta *et al.*, 2006). However, the effects of AR inhibition were limited to patients with moderate increases in HbA1c values (Hotta *et al.*, 2006). The central role of AR in diabetic neuropathy has been confirmed by experiments using AR-knockout (AR-KO) mice which are protected from neuropathy when made diabetic (Ho *et al.*, 2006), while AR-overexpressing mice exhibited more severe neuropathy than wild-type (WT) diabetic mice (Yagihashi *et al.*, 2001). Subsequent studies indicated, however, that severe hyperglycaemia and long durations of diabetes could initiate neuropathy even in AR-KO mice. It is therefore likely that mechanisms independent of polyol pathway flux also operate in the progression of diabetic neuropathy.

Although less explored, increased flux through the hexosamine pathway has been proposed as an additional contributor to the pathogenesis of diabetic neuropathy (Yagihashi, 2016; Feldman *et al.*, 2017). Excess glucose drives glycolysis and conversion of glucose-6-phosphate to fructose-6-phosphate (F6P). Two to 5% of F6P is diverted into the hexosamine biosynthetic pathway (HBP), via conversion to glucosamine-6-phosphate (GlcN6P) by the rate limiting enzyme, glutamine-fructose-6-phosphate amidotransferase (GFAT). GlcN6P is then irreversibly converted to the end-product of the HBP, UDP-N-acetylglucosamine, which serves as the substrate for post-translational modification of proteins by covalent O-linked addition of N-acetylglucosamine glycosylation (O-GlcNAcylation). Excessive O-GlcNAcylation of

nuclear/cytosolic proteins in diabetes has been linked with insulin resistance and cell dysfunction (Slawson *et al.*, 2010; Hardivillé and Hart 2014; Semba *et al.*, 2014). While the HBP pathway is regulated by allosteric feedback from UDP-N-acetylglucosamine to inhibit GFAT, GlcN (amino monosaccharide glucosamine) once produced or exogenously given, bypasses GFAT as it is directly phosphorylated to generate GlcN6P, likely resulting in aberrant biological reactions. Indeed, a pathogenic role for HBP was recently proposed in both animal models of diabetic retinopathy (Semba *et al.*, 2014) and cultured mesangial cells used to model diabetic nephropathy (Masson *et al.*, 2006). In contrast, although GlcN was found to be toxic to cultured motor neurons (Lim *et al.*, 2010), its relationship to diabetic neuropathy has not been adequately addressed. Interestingly, some studies have connected endoplasmic reticulum (ER) stress with HBP and the genesis of diabetic complications (Werstuck *et al.*, 2006; Moore *et al.*, 2016). A role for ER stress in the development of neuropathy was confirmed by several laboratories using streptozotocin-induced diabetic rats and CCAT-enhancer-binding protein-beta CCAT-enhancer-binding homologous protein (CHOP)-deficient mice (Lupachyk *et al.*, 2013; Wu *et al.*, 2013).

In this study, we performed a comprehensive metabolomics analysis of peripheral nerves from diabetic AR-KO mice and identified GlcN as a candidate trigger of neuropathy. We further attempted to clarify how GlcN influences peripheral nerve.

Materials and methods

Evaluation of neuropathy independent of polyol pathway in diabetic AR-deficient mice

AR-KO (Ho *et al.*, 2006) and WT (C57Bl/6J) (WT) mice ($n = 16$ in each) were made diabetic at 8 weeks of age by intraperitoneal injection of streptozotocin (150 mg/kg) and followed for 16 weeks, with weekly monitoring of tail blood glucose and monthly determination of motor nerve conduction velocity (MNCV). Diabetes was confirmed by continuous glycosuria and hyperglycaemia (>300 mg/dl, 16.5 mmol/l). Non-diabetic mice served for comparison. Each group consisted of five animals. Measurement of MNCV followed the previously described method with near nerve temperature at 37°C controlled by a heating pad that was checked with a thermometer (Yagihashi *et al.*, 2001).

To elucidate the metabolic pathway responsible for neuropathy, AR-KO and WT mice with and without 12 weeks of diabetes were used for biochemical analysis. After killing the mice by decapitation, sciatic nerves (SNs) were dissected for metabolomics analysis and measurement of polyol concentrations. Nerve concentrations of sorbitol and fructose were measured by gas chromatography, as described previously (Yagihashi *et al.*, 2001).

All experiments were conducted in accordance with the Council Directive 2010/63EU of the European Parliament and the Council of 22 September 2010 on the protection of animals used for scientific purposes, and the Guideline for the Care and Use of Animals in our institutions (Hirosaki University School of Medicine and Tokyo Metropolitan Institute of Medical Science, 2011, approval number M14006).

Metabolomics analysis of SN in diabetic AR-KO mice

SN tissues of experimental mice with/without diabetes for 12 weeks were subjected to metabolomics analysis, which was undertaken at Human Metabolome Technologies, Inc. (Tsuruoka, Yamagata, Japan). Due to space limitations, detailed methods for the metabolomics analysis are described in the Supplementary_materials_and_methods. Briefly, bilateral SNs from four mice in each group were pooled and preserved at −80°C until use. Approximately 20 mg of frozen tissue was homogenized and the homogenate mixed with chloroform and water and centrifuged. The supernatant was concentrated after filtration and re-suspended in water for metabolomics analysis. The analysis was conducted by capillary electrophoresis time-of-flight mass spectrometry as a Basic Scan Package (Human Metabolome Technologies, Inc.) (Ohashi *et al.*, 2008; Ooga *et al.*, 2011). The spectrometer was scanned from material/charge ratio (*m/z*) 50–1000 (Ohashi *et al.*, 2008). Peaks were extracted using automatic integration software to obtain peak information including *m/z*, peak area and migration time (MasterHands ver.2.9.0.9, Keio University, Tokyo) (Sugimoto *et al.*, 2012). Integrated areas of the annotated peaks were then normalized to an internal standard as the relative area that represented concentration of the metabolites (Soga *et al.*, 2003). Detected metabolites were plotted on metabolic pathway maps using VANTED software (Junker *et al.*, 2006). Metabolomics analysis was conducted three times using different samples from mice with comparable diabetic duration. Average values of relative area in each metabolite were subjected to between-group statistical analysis.

Cell survival and expressions of apoptosis signals and ER stress in Schwann cells exposed to GlcN

Methods of analysis of cell survival and expression of apoptosis signals and ER stress in Schwann cells exposed to glucosamine (GlcN: Sigma, St. Louis, MI) are described in the Supplementary_materials_and_methods.

Mitochondrial membrane potential, apoptosis-related proteins and oxidative stress in Schwann cells

Methods for the measurement of mitochondrial membrane potential (MMP), expression of apoptosis-related

proteins and oxidative stress in Schwann cells exposed to GlcN are described in the Supplementary_materials_and_methods.

Glucose uptake

IMS32 Schwann cells were starved in serum-free medium for 12 h and subsequently stimulated with 1 mM/l insulin for 16 min. Glucose uptake was determined by enzymatic photometric assay using a 2-deoxyglucose uptake measurement kit (COSMO BIO Co. Ltd., Tokyo, Japan) (Saito *et al.*, 2011). One μM/l cytochalasin was used as an inhibitor of glucose uptake.

Expression of hexokinase, ER stress, ATP content and cell proliferation signals in Schwann cells

GlcN is known to be metabolized to GlcN6P by mitochondrial hexokinase (Hex) after incorporation into cells (Buse, 2006; Slawson *et al.*, 2010). We therefore examined the expression of Hex-I and -II after separation of mitochondrial and cytosolic fractions from cultured Schwann cells exposed to 5.6 and 30 mM glucose with or without 10 mM GlcN by western blot analysis. Fractionation was conducted using a mitochondria/cytosol fractionation kit (BioVision, Inc.) using a previously described method (Wieckowski and Wojtczak, 2015). Primary specific antibodies against Hex-I and -II (both Cell Signaling Technology), and heat shock protein 60 (Santa Cruz Biotechnology) as markers of mitochondrial proteins were applied to the transferred membrane of SDS–PAGE at room temperature for 2 h.

To determine whether upregulation of hexokinase I (Hex-I) correlated with increased expression of cleaved caspase 3 (CC3), Schwann cells were co-treated with 10 mM GlcN and Hex-I siRNA or scrambled siRNA as a control. CC3 expression was examined by western blot as described above. Stealth siRNAs targeting mouse Hex-I were purchased from Thermo Fisher, Inc. (Schindler and Foley, 2013). Transfection of duplex siRNA was performed using Multifectom (Promega Co.) according to the manufacturer's protocol. In brief, siRNA was diluted into 1 pM/μl with opti MEM-I (Thermo Fischer, Inc.). Diluted siRNA was mixed with Multifectom, which was added into the medium for transfection. Two days after transfection, the efficacy of knock down was assessed by western blotting. After confirmation of Hex-I knock down, Schwann cells were stimulated with 10 mM GlcN for 24 h, then expression of CC3 evaluated by western blot. Reproducibility of the results was confirmed by repeated blot analysis. To determine whether enhanced Hex-I expression in mitochondria gave rise to altered ATP production, we measured ATP content of GlcN-exposed cells and compared it with unexposed cells. ATP content was measured by Luciferase–Luciferin reaction method using an ATP measurement kit for cells (Toyo Ink, Tokyo, Japan) as described previously (Manfredi *et al.*, 2002). Protein concentration was measured by the Bradford method.

To determine the effects of GlcN on cell proliferation signals in Schwann cells, expression of Akt (Cell Signaling Technology), phosphorylated Akt (p-Akt) (Cell Signaling Technology), phosphorylated S6RP (Cell Signaling Technology) and (cyclin-dependent kinase inhibitor 1B) (Santa Cruz Biotechnology) were examined by western blot analysis as described previously (Tsuboi *et al.*, 2016). All experiments were repeated at least three times and expression levels were quantified by densitometric analysis normalized to β-actin levels. Average values were compared between GlcN-added and GlcN-free groups.

Effects of PUGNAc on GlcN toxicity

O-linked addition of N-acetylglucosamine is known to contribute to posttranslational protein modification of the nucleus and cytosol, which plays an important role in cell function (Slawson *et al.*, 2010: Semba *et al.*, 2014). To explore the role of O-GlcNAcylation of proteins in injury of Schwann cells exposed to GlcN, PUGNAc [O-(2-acetamido-2-deoxy-D-glucopyranosylidene) amino N-phenylcarbamate] (Sigma Aldrich), an inhibitor of O-GlcNAcase which breaks down O-linked addition of N-acetylglucosamine from glycosyl-binding serine and threonine residues (Mehdy *et al.*, 2012), was applied for 24 h to cultured Schwann cells prior to GlcN treatment to determine whether PUGNAc enhances the cytotoxic effects of GlcN on the Schwann cells. After exposure to GlcN with addition of 100 μM PUGNAc, cell survival of Schwann cells and expression of CC3 was evaluated using a cell counting kit 8 (Dojindo) and western blot analysis as described above, respectively. The experiments were repeated at least three times to confirm the reproducibility of the results and the average values of cell survival rate and the extent of CC3 expression measured by densitometric analysis were compared between groups.

GlcN effects on neurite growth and survival of dorsal root ganglion neurons

Effects of GlcN on neurite growth and survival of dorsal root ganglion neurons were evaluated by methods described in the Supplementary_materials_and_methods.

In vivo effects of GlcN on peripheral nervous system in mice

After overnight fast, non-diabetic healthy 8-week-old C57BL/6J mice (body weight ~30 g) ($n = 20$) were anesthetized with isoflurane. Saline or GlcN at a dose of

0.17 g/kg (~10 mM *in vivo*) was slowly injected into the jugular vein. To determine the preventive effects of an ER stress inhibitor or an ATP donor, 4-phenylbutyrate (4PB) or inosine, was intraperitoneally given at a dose of 10 or 200 mg/kg to the mice, either 16–18 h or 60 min before GlcN administration, respectively. Each group consisted of five animals. Following 15 min of GlcN infusion, animals were killed by decapitation and SNs were removed, homogenized and used for measurements of Na, K-ATPase activity, ATP content and expression of Hex in the mitochondrial and cytosolic fractions by western blot analysis. Na, K-ATPase activity was measured by conventional methods as described previously (Nishizawa *et al.*, 2010). ATP measurement was performed as described above (Manfredi *et al.*, 2002) and western blot analyses were conducted using specific antibodies.

To determine the long-term effects of GlcN on peripheral nerves, Alzet® osmotic minipumps (Durect Corp., Cupertino, CA, USA) were surgically implanted at the nape of the neck via a 1 cm opening in the skin of AR-KO ($n = 10$) and WT ($n = 10$) mice under isoflurane anaesthesia. Before implantation, the minipumps were primed with 4.8 mg/ml (1 M) GlcN solution. Each pump delivered 0.15 µl (0.72 µg GlcN) per hour after placing them into 37°C physiological saline for a minimum of 4 h. Following insertion of the mini pumps, the skin was closed with surgical sutures, the wound was disinfected with povidone iodine and the animals received postoperative care. The mini pumps of control WT and AR-KO mice ($n = 5$ in each) were filled with physiological saline and were implanted by the same method. MNCV, sensory nerve conduction velocity and the tail flick test were performed at regular intervals for 12 weeks. MNCV and sensory nerve conduction velocity were measured in sciatic-tibial nerves under isoflurane anaesthesia and the measurement was conducted with near nerve temperature at 37°C, as controlled by a heating pad checked with a thermometer. The tail flick response to thermal stimulus was applied to test the heat perception threshold (Tail Flick Analgesia Meter, MK-330B, Muromachi Co., Tokyo, Japan) (Sugimoto *et al.*, 2008). Animals were killed by overdose of anaesthesia and foot pad skin was fixed with Zamboni's fixative overnight. Thereafter, 50 micron-thick frozen sections were subjected to immunostaining with protein gene product (PGP) 9.5 (for nerve fibres: Abcam) and collagen type IV (for basement membrane: Thermo Fischer) prior to evaluation of intraepidermal nerve fibre density by confocal laser scanning microscopy.

Statistical analysis

All quantitative data are expressed as group mean ± standard error with between group comparisons by analysis of variance with Bonferroni's *post hoc* corrections (SPSS, Inc., Chicago, IL, USA). Differences between groups were considered as significant when *P*-values were <0.05.

Data availability

The authors confirm that the data supporting the findings of this study are available within the article and its Supplementary materials.

Results

Neuropathy in AR-KO mice

Both AR-KO and WT mice showed consistently marked hyperglycaemia after induction of diabetes with streptozotocin (Fig. 1A). There was no difference in the levels of hyperglycaemia between diabetic AR-KO (AR-KO+DM) and diabetic WT (WT+DM) mice. Diabetes increased nerve sorbitol and fructose levels in WT mice (Fig. 1B). As expected, there was no increase in sorbitol in diabetic AR-KO mice, while there was a slight elevation of fructose in diabetic AR-KO mice compared to those in non-diabetic AR-KO and WT mice. As previously reported (Ho *et al.*, 2006), diabetic AR-KO were protected from significant MNCV slowing at 8 and 12 weeks of diabetes while MNCV in diabetic WT was significantly delayed as early as 4 weeks and up to 16 weeks after onset of diabetes (Fig. 1C). MNCV slowing in 16-week-diabetic AR-KO mice was comparable to that of diabetic WT mice (Fig. 1C). Thus, neuropathy develops independent of the polyol pathway after long durations of diabetes. We then sought the cause of neuropathy in AR-KO mice with 16-week diabetes.

Metabolomics analysis of AR-deficient mice (AR-KO)

Compared to non-diabetic AR-KO and WT mice, homogenized SN from diabetic AR-KO and diabetic WT mice with 12 week-diabetic duration yielded 12 (of a total of 213) upregulated metabolites (marked by red letters in Supplementary Table 1) with levels that were significantly greater by at least 1.5-fold in both diabetic AR-KO and diabetic WT mice (Supplementary Table 1 and Fig. 1). There was one downregulated metabolite (marked by green letters) which was less than 0.5-fold of non-diabetic AR-KO and WT mice. Metabolites of the glycolytic pathway such as glucose-6-phosphate and F6P were downregulated in non-diabetic AR-KO mice, whereas those in diabetic AR-KO mice were restored to levels in diabetic WT mice (Fig. 2 and Supplementary Fig. 1). The pathway from pyruvate to citric acid was not significantly altered in AR-KO mice with or without diabetes. The most remarkably upregulated metabolites were galacturonic acid, $NADP^+$, sarcosine, GlcN and isobutylamine (Fig. 2 and Supplementary Table 1), of which GlcN was the most prominent of the metabolites related to glycolysis.

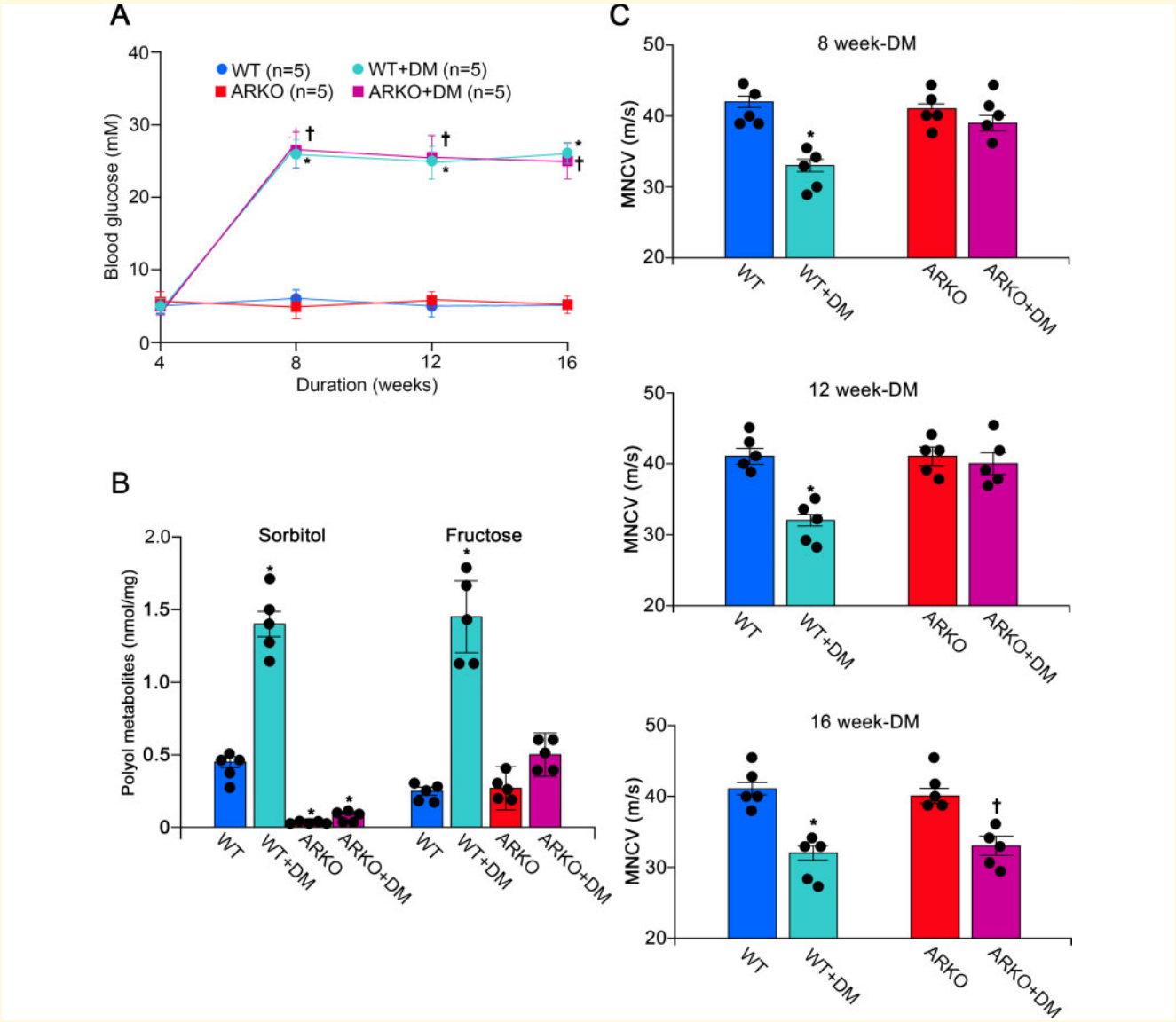

Figure 1 Development of neuropathic changes in AR-KO with increasing duration of diabetes. (**A**) Serial changes of blood glucose. (**B**) Nerve sorbitol and fructose concentrations. (**C**) MNCV at 8, 12 and 16 weeks of diabetes. Each group consists of five animals. WT; wild mice. WT+DM; diabetic wild mice, AR-KO+DM; diabetic AR-KO. Values of bars are expressed as mean ± standard error. *$P<0.01$ versus WT, †$P<0.01$ versus AR-KO.

Effects of GlcN on Schwann cell viability, apoptosis, ER stress and glucose uptake

Incubation of cultured Schwann cells with GlcN for 24 h yielded a significant and dose-dependent reduction in cell viability (Fig. 3A). Cell survival rate was not different between 5.6 and 30 mM glucose, indicating that high glucose did not itself affect the survival rate (Fig. 3B). By cell sorter assays, after 24-h exposure to 10 mM GlcN, either with 5.6 or 30 mM glucose, Schwann cells double positive with Annexin V and propidium iodide were significantly increased yielding ~40% of cell death (Fig. 3C). There was no difference in the population of double positive cells between 5.6 and 30 mM glucose. Concurrently, Schwann cells exposed to 1.5 and 10 mM GlcN showed robust expression of CC3 in a dose-dependent manner (Fig. 3D). Preincubation of Schwann cells with 10, 20 and 40 μM Z-VAD-FMK, an apoptosis inhibitor, successfully reduced CC3 expression in a dose-dependent manner. Co-incubation with either N-acetylcysteine as an antioxidant, or 4PB as an ER stress inhibitor did not significantly influence the expression of CC3, whereas inosine as an ATP donor suppressed CC3 expression (Fig. 3E). GlcN exposure significantly suppressed both 2-deoxyglucose uptake into Schwann cells

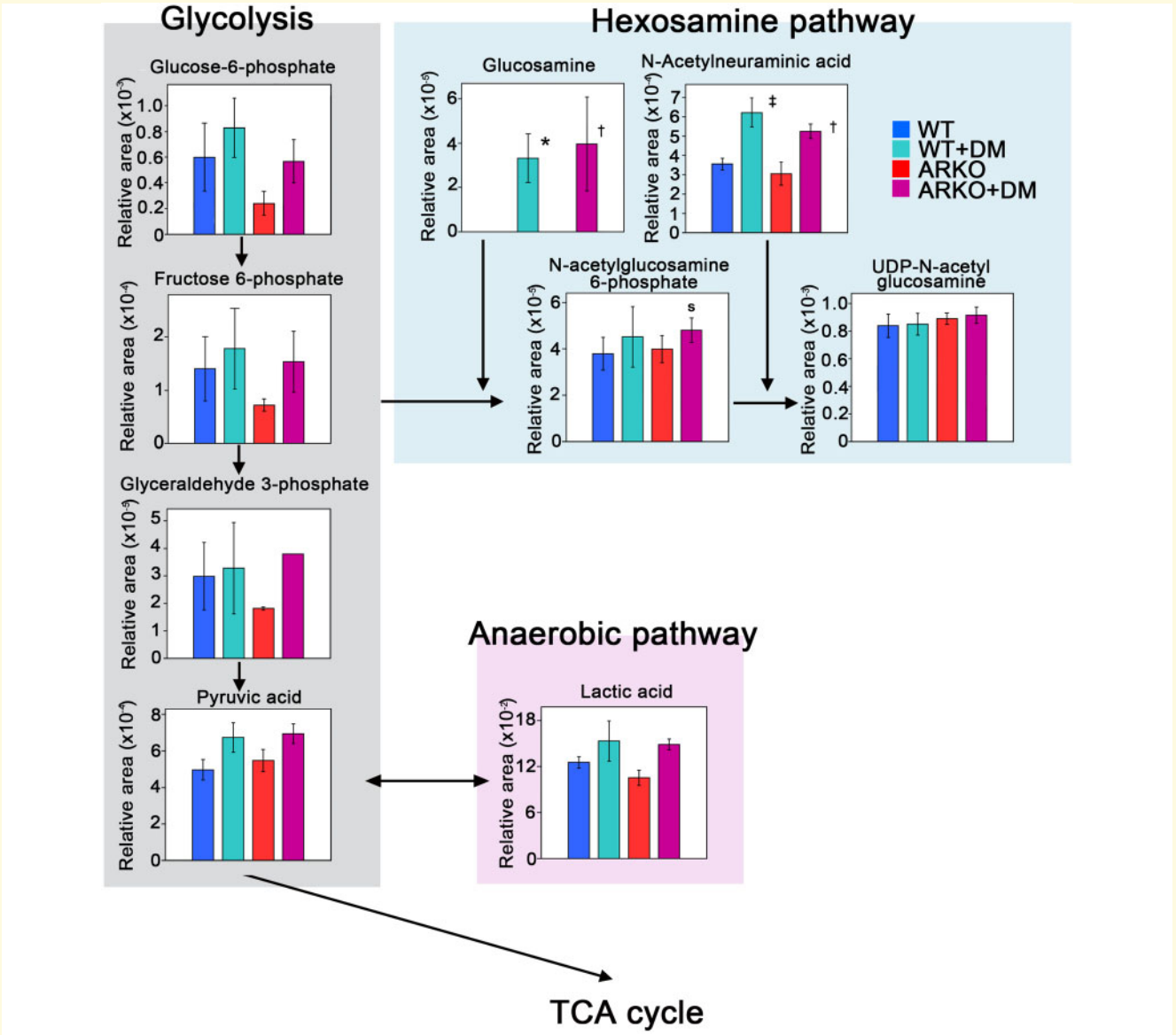

Figure 2 Metabolomics analysis of SN in mice with/without diabetes (see also Supplementary Table 1 and Fig. 1). Alteration of major metabolites related to glycolytic pathways detected by metabolomics analysis is illustrated. We found a marked increase in GlcN in both diabetic wild (WT+DM) and diabetic AR-knockout mice (AR-KO+DM) compared to non-diabetic AR-KO and WT. More details of related pathways are shown in Supplementary Table 1 and Fig. 1. The analysis was repeated three times using different animals and the average values were subjected to statistical analysis. Bar stands for mean ± standard error. *$P<0.01$ WT versus WT+DM, †$P<0.01$ AR-KO versus AR-KO+DM, ‡$P<0.05$ WT versus WT+DM, §$P<0.05$ AR-KO versus AR-KO+DM. See also Supplementary Table 1 for the metabolite list. G1P, glucose-1-phosphate; G6P, glucose-6-phosphate; F6P, fructose-6-phosphate; Glc-6P, glucosamine-6-phosphate; NAcGlcNP, N-acetylglucosamine-phosphate.

and insulin-induced glucose uptake (Supplementary Fig. 2A). GlcN exposure also elicited enhanced expression of CHOP and activating transcription factor 4, which were suppressed by co-treatment with 4PB or inosine, but not with N-acetylcysteine (Supplementary Fig. 2Ba–c). Final conditions of the medium were pH 7.68 in control, pH 7.69 in 1 mM GlcN and pH 7.62 in 10 mM GlcN and pH adjustment did not alter the results (data not shown).

MMP, apoptosis-related proteins and reactive oxygen species in Schwann cells

MMP in cultured Schwann cells, as measured by rhodamine 123 uptake ($\Delta\Phi$), was significantly reduced when the cells were exposed to 10 mM GlcN, while there was no difference in MMP between 5.6 and 30 mM glucose (Fig. 4A and B). In conjunction with the suppressed

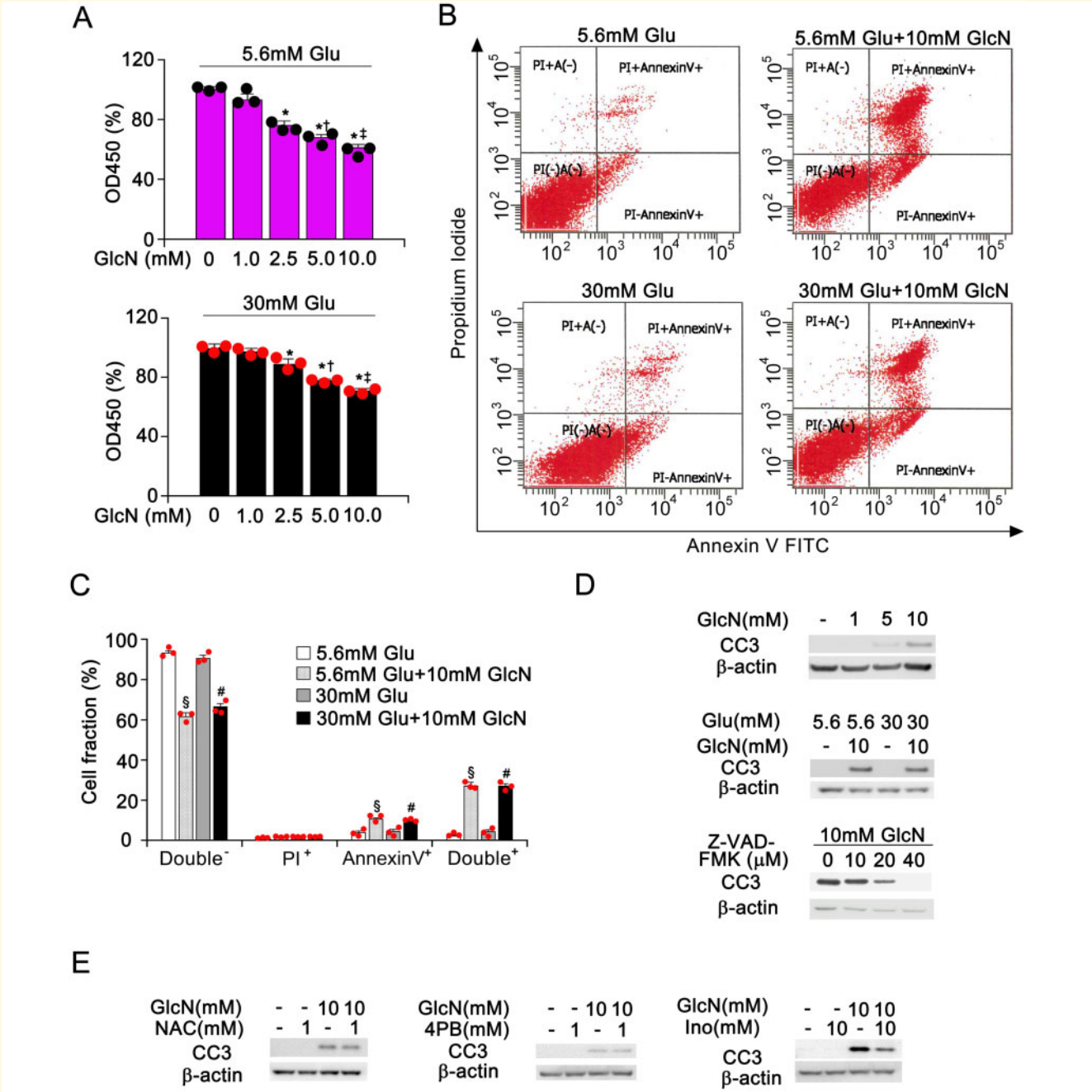

Figure 3 Accelerated cell death of Schwann cells exposed to GlcN. (**A**) MTT assay. (**B**) Cell sorter assay on apoptotic cells labelled with Annexin V and propidium iodide. (**C**) Quantification of apoptotic cells. (**D**) Expression of CC3 and effect of apoptosis inhibitor Z-VAD-FMK by western blot (uncropped blots can be seen in Supplementary Figs 3 and 4). (**E**) Effects of antioxidant, N-acetylcysteine and ER stress inhibitor, 4PB and ATP donor, inosine (Ino) on the expression of CC3. Experiments were repeated three times. Values are expressed as mean ± standard error. $^{*}P<0.01$ versus 0 mM GlcN, $^{\dagger}P<0.05$ versus 1.0 mM GlcN, $^{\ddagger}P<0.01$ versus 2.5 mM GlcN, $^{\S}P<0.01$ versus 5.6 mM glucose (Glu), $^{\#}P<0.01$ versus 30 mM Glu.

MMP, real time quantitative PCR analysis showed that mRNA expression of proapoptotic proteins such as Bad and Bnip3L/Nix in mitochondria were all elevated in Schwann cells exposed to GlcN (Fig. 4C). There was no difference in the expression of these molecules in the presence of 5.6 or 30 mM glucose.

As expected, nearly 100% cultured Schwann cells exposed to 0.5 mM H_2O_2 stained positive for reactive oxygen species (ROS) indicator CellRox^{TM}, whereas cells free from H_2O_2 were mostly negative (Fig. 4D). With incubation of 5.6 mM glucose, 85% of cell was ROS-positive and this increased to nearly 90% when cells were

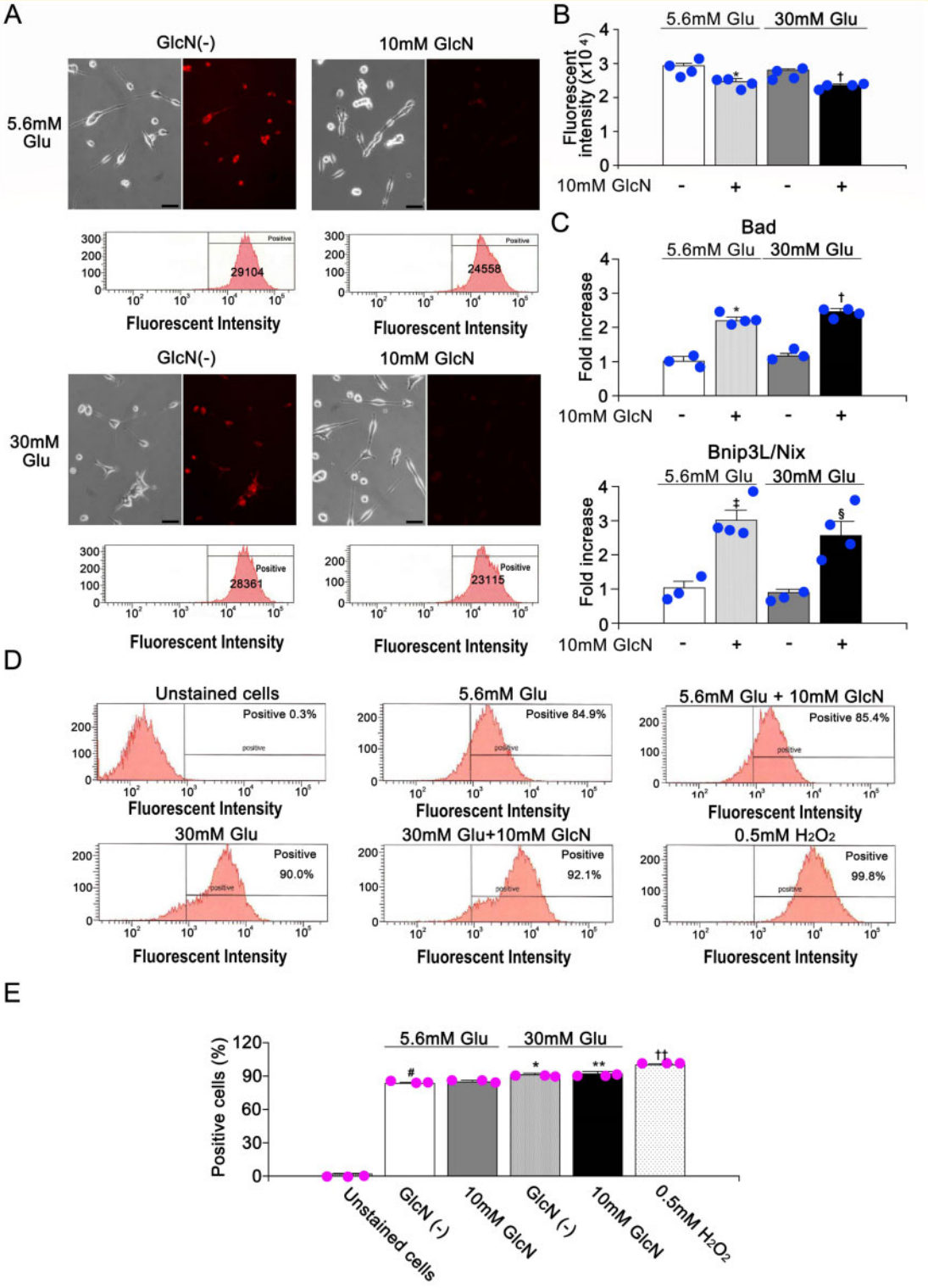

Figure 4 Reduced MMP of Schwann cells exposed to GlcN and oxidative stress. (**A**) Left panel exhibits phase contrast image of injured Schwann cells and right panel discloses lowered MMP shown by red fluorescence (scale bar indicates 50 μm). (**B**) Quantification disclosed significant reduction in MMP in GlcN-exposed cells. (**C**) RT-PCR analysis detected elevated mitochondrial apoptotic protein Bad and Bnip3L/Nix in GlcN-exposed Schwann cells. (**D**) Cell population positive for oxidative stress marker CellRox by cell sorter analysis. Addition of 10 mM GlcN did not increase the population of oxidative stress-positive cells. (**E**) Quantitation did not yield significant increases in CellRox-positive cells when exposed to 10 mM GlcN. Experiments were repeated 4 times. Values are expressed as mean ± standard error. *$P<0.01$ versus GlcN(−)/5.6 mM Glu, $^{\dagger}P<0.01$ versus GlcN(−)/30 mM Glu, $^{\ddagger}P<0.05$ versus GlcN(−)/5.6 mM Glu, $^{\S}P<0.05$ versus ND, $^{\#}P<0.01$ versus unstained cells, **$P<0.01$ versus 0.5 mM H_2O_2.

exposed to 30 mM glucose. The addition of 10 mM GlcN to either 5.6 or 30 mM glucose did not further increase the population of cells positive for ROS (Fig. 4E).

Hexokinase, ER stress, ATP content and cell proliferation signals in Schwann cells

GlcN is incorporated into cultured Schwann cells to be converted to GlcN6P by hexokinase (Hex)-I. Western blot analysis revealed markedly elevated expression of Hex-I in the mitochondrial fraction, but not in the cytosolic fraction of GlcN-exposed Schwann cells (Fig. 5A). On the other hand, Hex-II expression was not significantly altered at either 5.6 or 30 mM glucose (Fig. 5B). Association of cell death and CC3 expression with enhanced Hex-I expression was confirmed by a marked inhibition of CC3 expression and cell death when pretreated with siRNA for Hex-I (Fig. 5C). Enhanced expression of CHOP or activating transcription factor 4 as ER stress signals was also suppressed by pretreatment with Hex-1 siRNA (Supplementary Fig. 2C). Measurement of ATP content in Schwann cell homogenates demonstrated a marked reduction of ATP in cells exposed to GlcN, which was significantly recovered ~70% by pretreatment with inosine or siRNA of Hex-I (Fig. 5D).

Exposure of Schwann cells to GlcN significantly suppressed the expression of proliferation signals p-Akt and pS6RP, and also enhanced expression of the anti-proliferation signal cyclin-dependent kinase inhibitor 1B. This pattern was similar whether cells were exposed to either 5.6 or 30 mM glucose (Fig. 5E). Densitometric analysis confirmed the suppressive effects of GlcN on these molecules (Fig. 5F).

O-GlcNAcylation in GlcN cytotoxicity

Protein O-GlcNAcylation was confirmed in cultured Schwann cells and was enhanced by pretreatment with PUGNAc in Schwann cells exposed to GlcN (Fig. 6A). O-linked addition of N-acetylglucosamine of Schwann cells free from GlcN was not influenced by PUGNAc treatment. Schwann cell survival was significantly reduced when treated with GlcN, but PUGNAc pretreatment did not further worsen the survival of GlcN-treated cells (Fig. 6B). There was no significant difference in the effect of PUGNAc treatment on cell survival between 5.6 and 30 mM glucose. The expression of CC3 in GlcN-treated Schwann cells was reduced when pretreated with PUGNAc, and the effects of PUGNAc were not different between 5.6 and 30 mM glucose (Fig. 6C).

GlcN effects on dorsal root ganglion neurons

After 48 h in culture with conditional serum-free medium in the presence or absence of 1 mM GlcN, nearly 50% of dorsal root ganglion neurons extended neurites (Fig.7A). In contrast, the number of neurite-bearing cells and average neurite length were blunted in neurons exposed to 10 mM GlcN (Fig. 7A and D). Prolonged exposure of neuronal cells to 10 mM GlcN caused a significant decrease in the population of viable neurons after 3 or 6 days of culture (Fig. 7B and E). Treatment with 1 mM GlcN had no significant effects at 3 days, but slightly reduced the survival after 6 days of culture. Consistent with the effect on cultured Schwann cells, exposure of neurons to 1 mM GlcN and 10 mM GlcN for 3 days elicited robust expression of CC3 in the cytoplasm or occasionally in the nucleus (Fig. 7C). Quantitation of neurite-bearing cells and neurite length revealed a significant reduction of these indices in GlcN-exposed neurons at a dose of 10 mM, but there was no significant effect at a dose of 1 mM (Fig. 7D). Culture medium pH was comparable between control and 1 mM GlcN or 10 mM GlcN and the effect of high osmolality on cell survival at 7 days was much smaller, $55 \pm 7\%$, in 10 mM mannitol at 7 days compared to $12 \pm 2\%$ of 10 mM GlcN (versus control $79 \pm 5\%$), indicating potent cytotoxicity of 10 mM GlcN.

In vivo effects of GlcN on peripheral nervous system in mice

Ouabain sensitive Na, K-ATPase activity of SN homogenates was significantly reduced in mice injected with a single dose of GlcN (Fig. 8A). Treatment with inosine slightly, but significantly, restored its activity, while the effect of 4PB was obscure. Ouabain insensitive Na, K-ATPase activity was comparable among all groups. Concurrently, there was a marked reduction of ATP content in the SN of GlcN-injected mice, which was restored in inosine-treated mice but not in the 4PB-treated group (Fig. 8B). In contrast to *in vitro* Schwann cells exposed to GlcN, dissected SNs from GlcN-injected mice did not show enhanced expression of CHOP and there was no apparent influence of inosine or 4PB on the expression (Supplementary Fig. 2D). As in *in vitro* conditions, Hex-I was mainly expressed in the mitochondria-rich fraction in the SN, but to a lesser extent was also found in the cytosolic fraction, while liver tissues did not contain this enzyme (Fig. 8C). Expression was enhanced nearly 3-fold in the mitochondrial fraction in GlcN-injected mice. The enhanced expression of mitochondrial Hex-I was not significantly affected by inosine pretreatment (Fig. 8D).

GlcN delivered via an osmotic pump did not influence body weight or blood glucose of either AR-KO or WT mice during the observation period (Fig. 8E). After 8 weeks of GlcN infusion, there were significant increases in thermal perception threshold using the tail flick test (Fig. 8F) along with significant MNCV and sensory nerve conduction velocity slowing in both AR-KO and WT mice (Fig. 8G and H). There were no significant differences in these parameters between AR-KO and WT mice with or without GlcN. Along with nerve dysfunction, there was significant

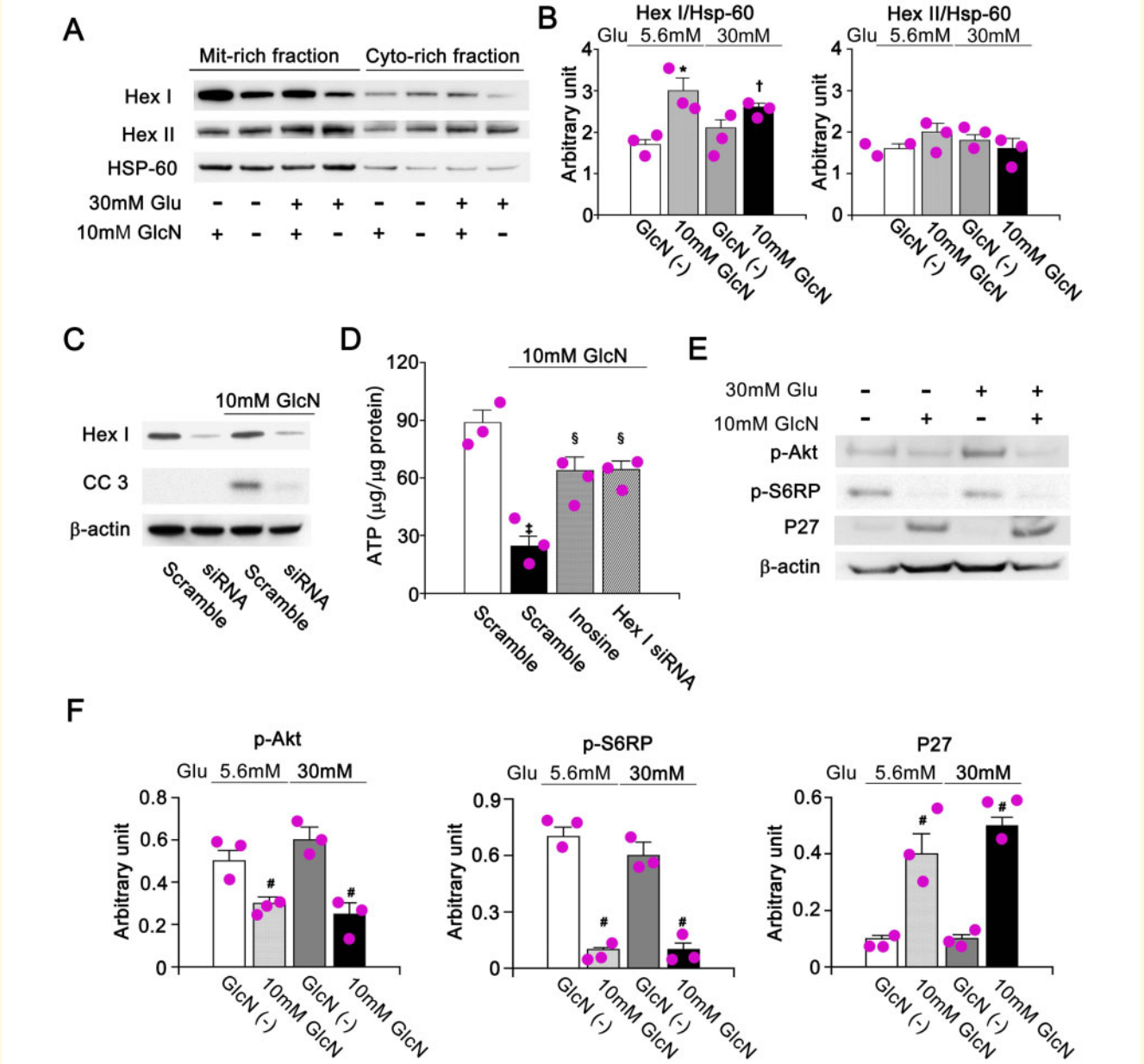

Figure 5 Augmented mitochondrial Hex-I expression and its inhibition by siRNA and expression of growth-related molecules. (**A**) Expression of Hex-I in mitochondrial fraction of Schwann cells. Heat shock protein 60 was control for mitochondrial fraction. (**B**) Densitometric analysis of Hex-I expression. (**C**) Effect of Hex-I siRNA on CC3 expression. (**D**) ATP concentrations in Schwann cells exposed to GlcN and effects of Inosine and Hex siRNA. (**E**) Expression of p-Akt, p-S6RP and p27 (cyclin-dependent kinase inhibitor 1B) of Schwann cells exposed to GlcN. (**F**) Densitometric analysis of cell proliferation signals. Experiments were repeated three times. Values are expressed as mean ± standard error. $^{*}P<0.05$ versus GlcN(−), $^{\dagger}P<0.05$ versus GlcN(−)/30 mM Glu, $^{\ddagger}P<0.01$ versus Scramble, $^{\S}P<0.05$ versus Scramble/10 mM GlcN, $^{\#}P<0.01$ versus GlcN(−). Uncropped blots can be seen in Supplementary Fig. 5.

reduction of intraepidermal nerve fibre density in either GlcN-infused AR-KO or WT mice compared to their respective control mice free from GlcN (Fig. 9A and B).

Discussion

In this study, we for the first time clearly demonstrated that GlcN accumulates in diabetic peripheral nerve. To separate the role of GlcN from other glycolytic pathways, such as the polyol pathway, we used AR-KO mice with longstanding diabetes to identify GlcN as a pathogenic candidate for diabetic neuropathy by comprehensive metabolomics analysis (Yagihashi *et al.*, 2001; Ho *et al.*, 2006). The hexosamine pathway (including GlcN) has long been suggested to be one of the major pathways for diabetic vascular complications, but it has not been

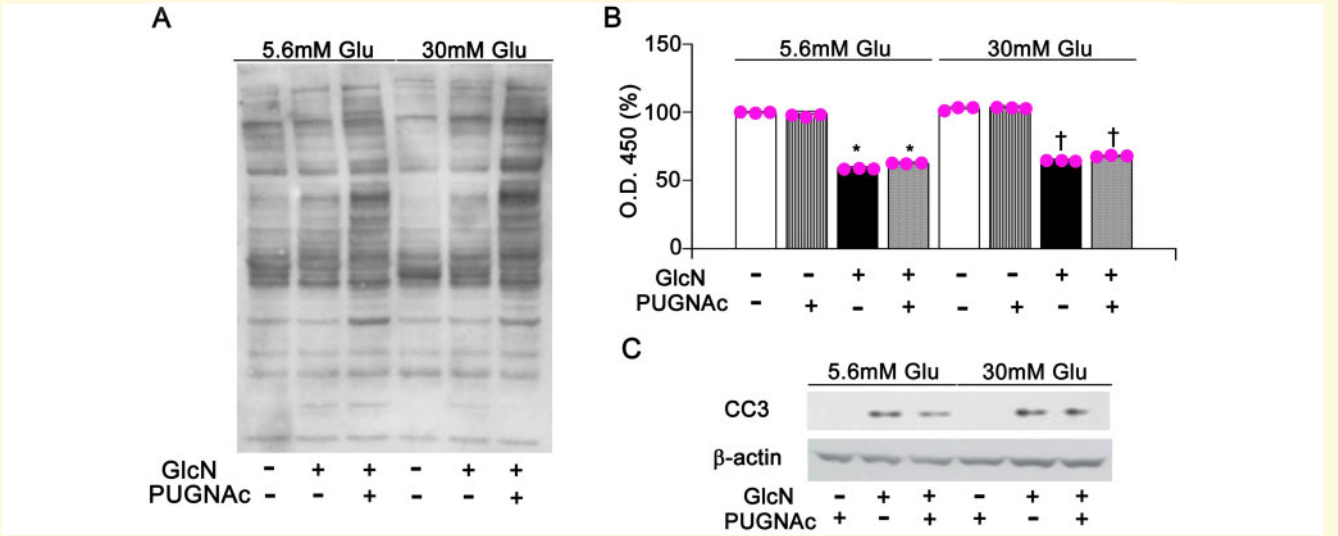

Figure 6 Effects of PUGNAC, an enhancer of O-GlcNAcylation, on the cell viability and CC3 expression in GlcN-exposed Schwann cells. (**A**) Augmented O-GlcNAcylation of structural proteins in the lane of PUGNAC pretreatment by SDS-electrophoretic gels. (**B**) Lack of further augmentation of reduced cell viability after PUGNAC-treatment. (**C**) Lack of augmentation of CC3 expression after PUGNAc treatment. Experiments were repeated three times. Values are expressed as mean ± standard error. *$P<0.01$ versus 5.6 mM, 5.6 mM + PUGNAc, †$P<0.01$ versus 30 mM, 30 mM + PUGNAc. Uncropped blots can be seen in Supplementary Fig. 6.

clearly distinguished from other glycolytic pathways that promote glycation/advanced glycation end-products formation, protein kinase C hyperactivity or mitochondria-derived oxidative stress (Brownlee, 2005; Slawson *et al.*, 2010; Semba *et al.*, 2014; Feldman *et al.*, 2017). In this study, we found that cultured Schwann cells exposed to GlcN showed accelerated cell death, increased expression of CC3, CHOP, mitochondrial Hex-I, Bad and Bnip3L/Nix along with lowered MMP and depletion of ATP. GlcN exposure also suppressed the expression of the cell proliferation signals pAKT and pS6RP in Schwann cells and impaired cell survival or neurite growth of isolated sensory ganglionic neurons. Consistent with *in vitro* effects, *in vivo* administration of GlcN to healthy mice-induced neuropathic changes which recapitulate the neuropathy encountered in animal models of diabetes (Yagihashi *et al.*, 2001; Nishizawa *et al.*, 2010; Feldman *et al.*, 2017). Taken together, our findings suggest that excessive GlcN contributes to the development of neuropathy in diabetes and may be a potential target of interventional treatment.

There are several possible metabolic pathways by which excessive GlcN flux may cause diabetes-specific complications. Hyperglycaemia-induced O-GlcNAcylation of nucleocytosomal proteins from F6P mediated by GFAT modifies gene transcription or cell function (Slawson *et al.*, 2010; Hardivillé and Hart 2014). In fact, mice transgenic for overexpression of GFAT, a rate-limiting enzyme of GlcN synthesis, or OGT (O-GlcNAcylation transferase), specifically in muscle and fat tissues, exhibit excessive O-linked GlcNAcylation of serine–threonine molecules with insulin resistance (McClain *et al.*, 1992; Hebert *et al.* 1996; Buse, 2006). Unfortunately, these investigators did not address whether these mice are susceptible to diabetic neuropathy. However, overexpression of GFAT in mesangial cells by adenovirus gene transfer caused increased expression of TGF-β and fibronectin, thereby recapitulating the alterations detected in glomeruli of diabetic animals (Weigert *et al.*, 2003). It is unlikely, that excessive O-GlcNAcylation contributed to the GlcN-induced nerve damage in our study because augmented O-GlcNAcylation after PUGNAC treatment did not worsen the deleterious effects on Schwann cells (see Fig. 6). Consistent with our results, independence of O-GlcNAcylation from tissue injury was also shown in retinal neurons (Nakamura *et al.*, 2001) as well as retinal Mueller cells (Moore *et al.*, 2016) when they were exposed to GlcN.

Excessive production of mitochondrial superoxide (ROS) has long been considered fundamental to diabetic vascular complications (Brownlee, 2005; Yagihashi, 2016; Feldman *et al.*, 2017). In our study, there was a slight but significant increase in ROS-positive cells exposed to 30 mM glucose, but no further increase after exposure to 10 mM GlcN. We could not find significant prevention of cell death or CC3 expression by the antioxidant N-acetylcysteine. It therefore seems unlikely that ROS play a major role in GlcN-induced nerve injury. An alternative explanation for GlcN toxicity may be induction of ER stress (Moore *et al.*, 2016), since involvement of ER stress has emerged as an important collateral glycolytic pathway that associates with occurrence of neuropathy in diabetic animals or animals fed with high fat diet (Lupachyk *et al.*, 2013; Wu *et al.*, 2013; O'Brien *et al.*,

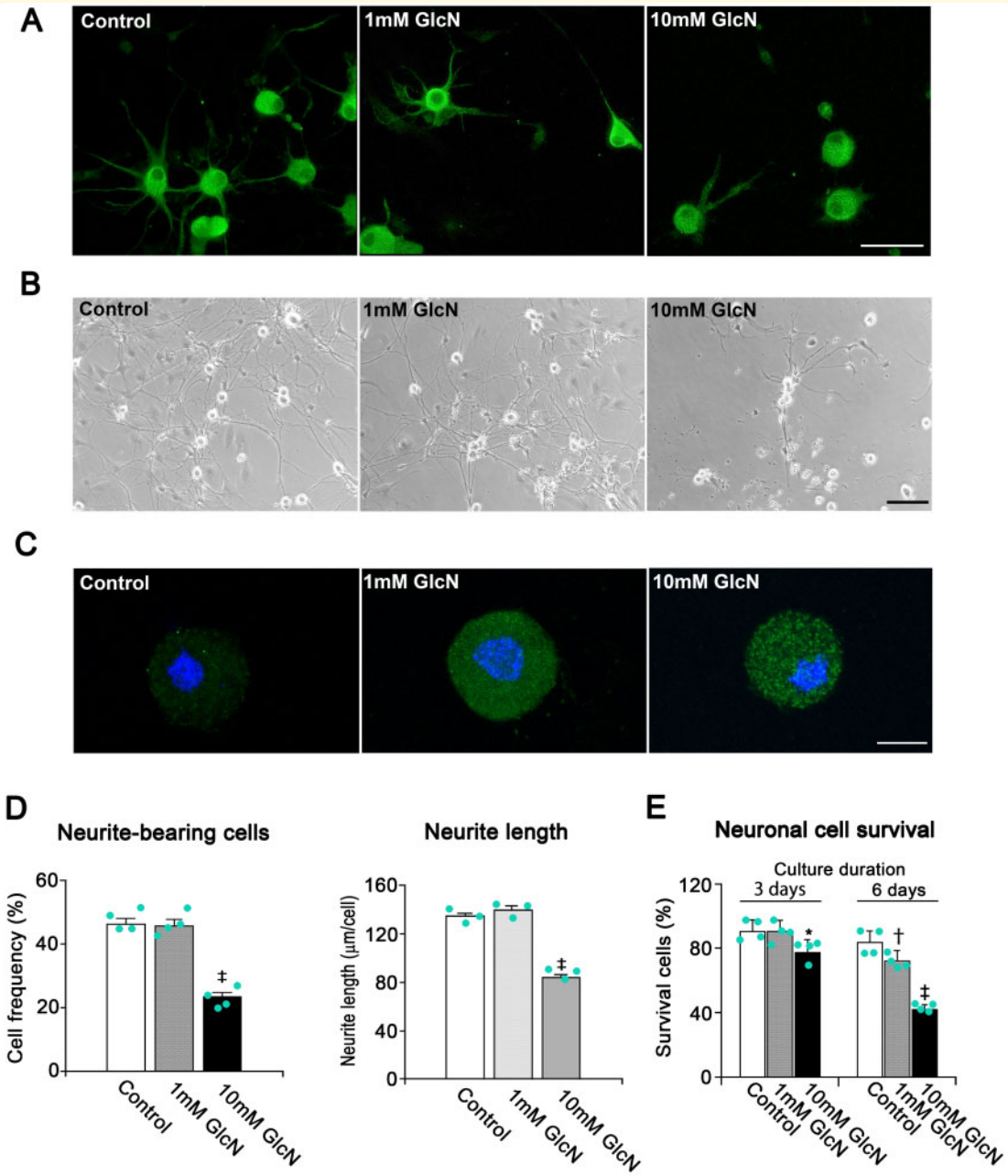

Figure 7 GlcN inhibited survival and neurite growth of cultured dorsal root ganglion neurons isolated from adult Wistar rats. (**A**) 10 mM GlcN exposure for 48 h caused reduction of neurite-bearing cells and suppressed neurite growth (immunofluorescence image of βIII-tubulin) (scale bar indicates 50 μm). (**B**) Phase contrast image of neuronal cell death after exposure to 1 or 10 mM GlcN for 48–72 h (scale bar indicates 100 μm). (**C**) Immunofluorescent expression of CC3; green in cultured neuronal cells exposed to GlcN (scale bar indicates 10 μm). Nuclei are stained blue with DAPI. (**D**) Significant reduction of neurite-bearing cells and reduced neurite length of neuronal cells exposed to 10 mM GlcN for 48 h. (**E**) Cell survival ratios determined by counting the number of viable neurons which possess phase-bright cell image at 3 days of culture, and by trypan blue staining at 6 days of culture, respectively. Survival ratios of neurons exposed to GlcN is progressively reduced in a dose-dependent manner. Experiments were repeated three to four times. Values of neurite-bearing cells are expressed as mean ± standard error. *$P<0.05$ versus Control, 1 mM GlcN, †$P<0.05$ versus control, ‡$P<0.01$ versus control, 1 mM GlcN.

2014). Wu and their colleagues described upregulated expression of ER stress markers such as increased CHOP/ORP150 ratio in the SN of high-fat diet and streptozotocin-induced diabetic rats (Wu *et al.*, 2013). An inhibitor of ER stress (TMAO) was found to suppress the development of neuropathy in diabetic rats fed with high fat diet (Lupachyk *et al.*, 2013). Consistent with these results, we also found increased expression of CHOP in Schwann cells exposed to GlcN (see Supplementary Fig. 2). However, we could not find any influence of the ER

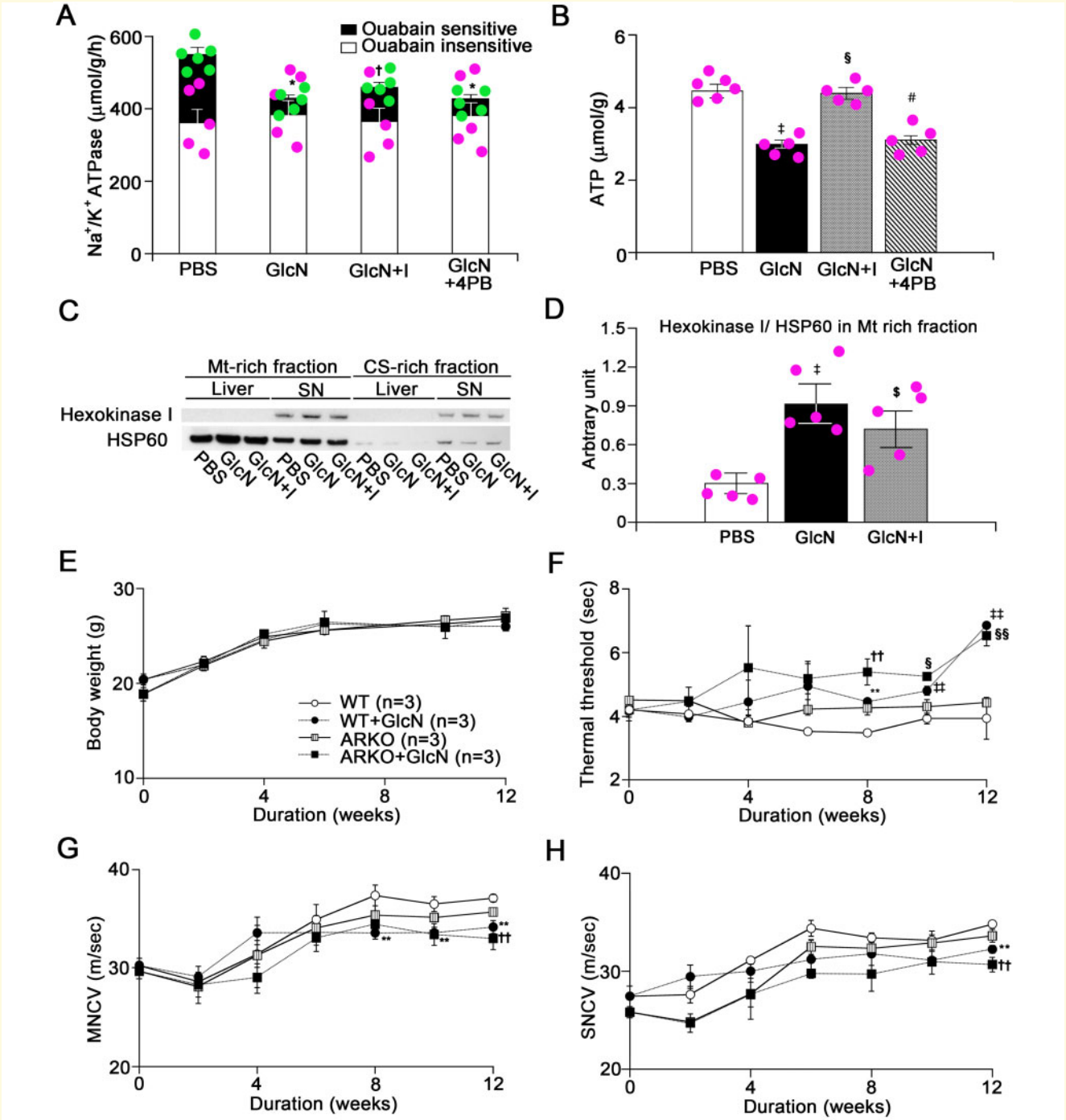

Figure 8 ***In vivo*** **effects of GlcN on peripheral nerve tissues in healthy mice.** (**A**) Marked reduction of ouabain-sensitive Na, K-ATPase activity in C57Bl/6J mice treated with 10 mM GlcN and effects of inosine (I) and ER stress inhibitor 4PB. (**B**) Significant reduction of ATP content in mice injected with GlcN and effects of I and 4PB. (**C**) Increased expression of Hex-I in mitochondria (Mt)-rich fraction from SN as well as cytosol (CS) to a lesser extent, while this enzyme was not contained in the liver. Uncropped blots can be seen in Supplementary Fig. 7. (**D**) Quantification of Hex-I expression in GlcN-injected mice and effect of I-treatment. (**E–H**) *In vivo* effects of GlcN on peripheral nerve of non-diabetic AR-deficient mice (AR-KO) and wild mice (WT) by an osmotic pump (0.17 g/kg/day, 1 µl/h) for 12 weeks. (**E**) Serial changes of body weight. (**F**) Significant elevation of thermal sensation threshold after 8 weeks in both AR-KO and WT given GlcN. (**G**) Delayed MNCVs in both AR-KO and WT given GlcN after 8 weeks. (**H**) Delayed sensory nerve conduction velocities in both AR-KO and WT given GlcN at 12 weeks. Values of bars are expressed as mean ± standard error. *$P<0.01$ versus phosphate buffered saline (Ouabain sensitive), $^{\dagger}P<0.05$ versus phosphate buffered saline, GlcN, GlcN+4PB (Ouabain sensitive), $^{\ddagger}P<0.01$ versus phosphate buffered saline, $^{\S}P<0.01$ versus GlcN, $^{\#}P<0.01$ versus phosphate buffered saline, GlcN+I, $^{\$}P<0.05$ versus phosphate buffered saline, **$P<0.05$ versus WT, $^{\dagger\dagger}P<0.05$ versus AR-KO, $^{\ddagger\ddagger}P<0.01$ WT, $^{\S\S}P<0.01$ versus AR-KO.

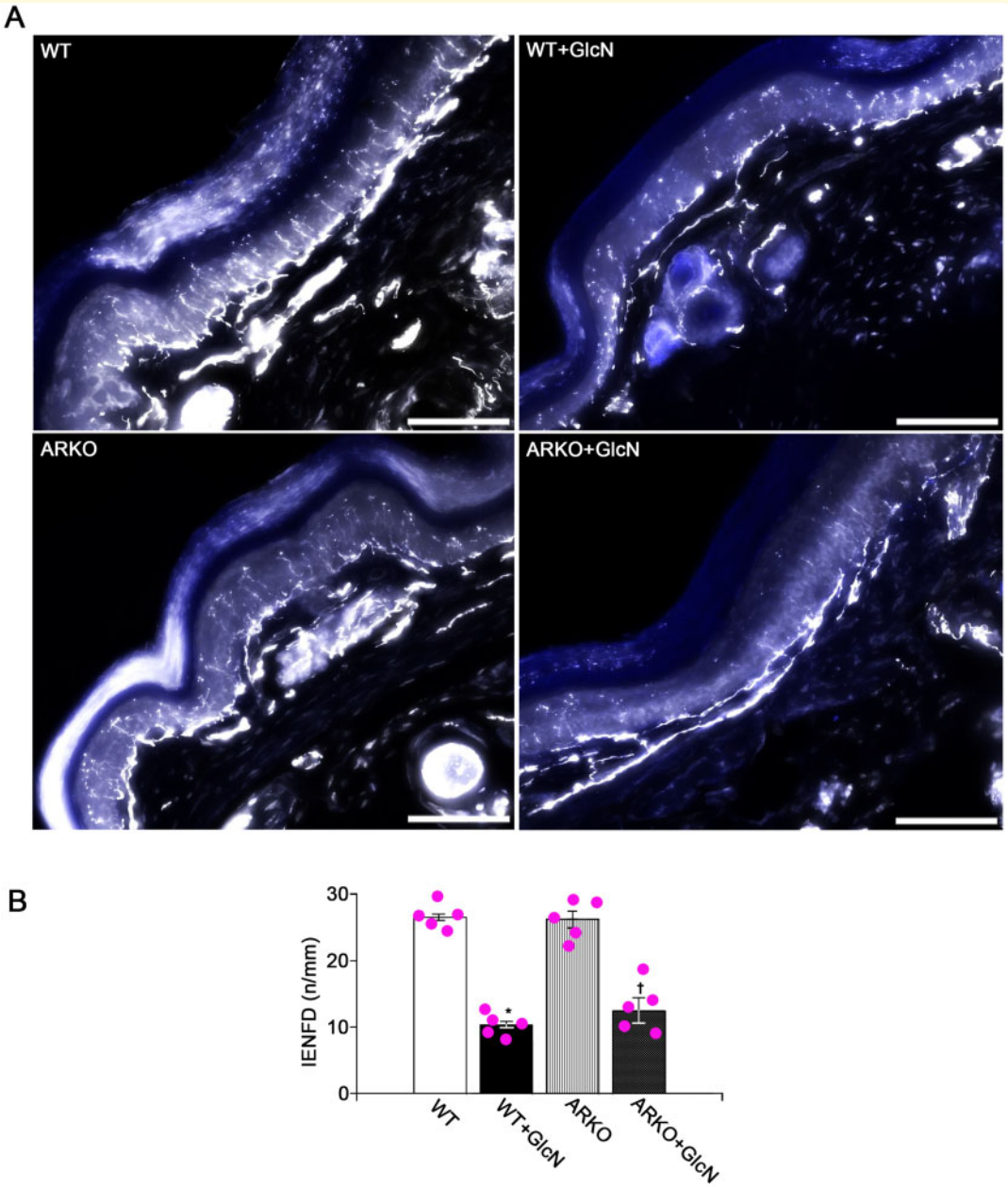

Figure 9 ***In vivo*** **effects of GlcN on peripheral nerve fibre morphology in healthy mice.** (**A**) Reduced intraepidermal nerve fibre density detected by immunohistochemical stains with protein G product 9.5 in both AR-KO and WT given GlcN for 12 weeks (scale bar indicates 200 μm). (**B**) Quantification of IENFD in AR-KO and WT given GlcN for 12 weeks and comparison with mice free from GlcN (N=5 mice). Bar stands for mean ± standard error. *P<0.01 versus WT, †P<0.01 versus AR-KO.

stress inhibitor 4PB on CC3 expression, indicating that ER stress may not be causally related to the GlcN-induced cell damage.

There has been a controversy regarding ATP depletion in GlcN-exposed tissues (Balkan and Dunning, 1994; Nakamura *et al.*, 2001). GlcN flux competitively inhibits glucose uptake, with downregulation of glucokinase expression in pancreatic β-cells or hepatocytes, resulting in induction of ER stress or apoptotic cell death (Kaneto *et al.*, 2001; Alejandro *et al.*, 2015). In this study, GlcN exposure caused robust depletion of ATP in peripheral nerve (Fig. 5D). Treatment with the ATP donor inosine successfully prevented Schwann cell death *in vitro*. Neurotoxic effects of GlcN previously shown in cultured motor neurons were related to energy depletion with loss of ATP and lowered glucose uptake (Lim *et al.*, 2010). Concurrently, we found increased Hex-I expression in Schwann cells exposed to GlcN or SNs of GlcN-injected mice. Correction of Schwann cell injury treated with Hex-I siRNA or the ATP donor inosine supports the

contention that poor energy production may contribute to GlcN-induced nerve damage, which mimics features of neuropathy in experimental diabetes (Yagihashi *et al.*, 2001; Akude *et al.*, 2011; Feldman *et al.*, 2017). Reduced energy production with altered AMP-kinase activity is fundamental to the progression of neuropathy in streptozotocin-induced diabetic animals (Roy Chowdhury *et al.*, 2012). Marked accumulation of GlcN detected in the SN of diabetic AR-KO mice suggests a pathogenic role of GlcN in the development of diabetic neuropathy.

Our results showing acute neurotoxicity of GlcN in cultured cells may be distinct from the late development of neuropathic changes in mice given GlcN. Most previous *in vitro* studies reported acute toxic effects of glycolytic products on Schwann cells or neuronal cells, but the results were not well validated *in vivo* and direct connections with neuropathy were not established. Consistent with the above, although exposure of cultured nerve cells to GlcN exerted robust molecular changes promoting apoptotic processes, it was hard to find nerve cell necrosis in animals with neuropathic changes. Nevertheless, follow-up of GlcN-infused animals demonstrated slow development of impaired heat-evoked responses, nerve conduction slowing and loss of small sensory nerve fibres in the skin. Such slowly developing changes of nerve function and structure may reflect the pathogenic role of GlcN in the slow progression of diabetic neuropathy. Currently, despite the robust accumulation of GlcN in nerve from both WT and AR-KO mice with longstanding diabetes, the precise metabolic pathway driving GlcN accumulation is yet to be established.

In this study, we concentrated our metabolomics analysis on the glycolytic pathway and candidates were selected from the substances that increased by 1.5 times or greater in diabetic AR-KO and WT mice compared to their non-diabetic counterparts. We did not specifically investigate the role of sarcosine or acetoacetamide, which were also altered in diabetic AR-KO mice. However, these products appeared to be far from the glycolytic pathway. In addition, we do not know the exact source of excessive GlcN in the hyperglycaemic milieu, although both extracellular and intracellular concentrations of GlcN should be high in diabetic mice (Buse, 2006). Recently the concept that insulin resistance in peripheral nerve is involved in development of diabetic neuropathy has been proposed (Grote *et al.*, 2011; Zochodne, 2016). Indeed, impaired phosphorylation of insulin receptor substrate is associated with nerve conduction slowing in streptozotocin-induced diabetic animals (Grote *et al.*, 2011; Tsuboi *et al.*, 2016). Further analysis may be warranted to solve the question of whether insulin resistance is *per se* involved in GlcN-induced neuropathy.

GlcN is known to be popular as a supplement for the remedy of arthritis, rheumatic joint disease and age-related locomotive disorders. Our results may prompt some alarm at the overuse of GlcN as a dietary supplement. However, the dose used as a supplement is much smaller compared to the dose applied in this study, although the mode of intestinal absorption, metabolic sequelae and excretion are mostly open to question. It is unlikely that daily intake of GlcN is causally related to unwanted effects. Nevertheless, it may be wise to avoid excessive consumption of GlcN in patients with long-term diabetes.

There are some limitations to this study. First, we identified GlcN among 213 candidate substances from the metabolomics analysis, but there might be other metabolites that should also be evaluated for their toxicity. Second, a reliable method for measurement of tissue concentrations of GlcN is yet to be established and it is not known how blood and tissue concentrations of GlcN are regulated. Our preliminary efforts to measure blood concentrations of GlcN are now underway and hopefully the method will be applicable to clinical use in near future. In addition to the above, the characterization of metabolites by metabolomics analysis was often insufficient for distinction from other similar metabolites. Chemical isomers or heterolytic substances may be included in the metabolomics substrates. In conclusion, we identified the GlcN pathway as an important mediator of diabetic neuropathy during long-term hyperglycaemia using AR-KO mice. Chronic application of GlcN reproduced the peripheral nerve injury encountered in diabetes. Our results may explain the reason why a single treatment strategy has not been successful for the treatment of neuropathy in diabetes.

Supplementary material

Supplementary material is available at *Brain Communications* online.

Acknowledgements

Technical assistances of Wataru Inaba, Misato Sakamoto, Hiroko Mori and Rumiko Imai are greatly appreciated. Contributions of students (Arisa Suzuki, Eriko Otsu, Azusa Kakuta, Yuki Takeuchi) are also appreciated. We also thank Professor Nigel Calcutt, Department of Pathology, University of California, San Diego, USA for his critical review of this manuscript and special advice throughout the study.

Funding

This study was supported by grants in aid from the Ministry of Science, Education, Culture and Sports (16K09771 to S.Y.) and the Ministry of Health and Welfare (S.Y.), Japan.

Competing interests

The authors report no competing interests.

References

Akude E, Zherebitskaya E, Chowdhury SK, Smith DR, Dobrowsky RT, Fernyhough P. Diminished superoxide generation is associated with respiratory chain dysfunction and changes in the mitochondrial proteome of sensory neurons from diabetic rats. Diabetes 2011; 60: 288–97.

Alejandro EU, Bozadjieva N, Kumusoglu D, Abdulhamid S, Levine H, Haataja L, et al. Disruption of O-linked N-acetylglucosamine signaling induces ER stress and β cell failure. Cell Rep 2015; 13: 2527–38.

Balkan B, Dunning BE. Glucosamine inhibits glucokinase *in vitro* and produces a glucose-specific impairment of the *in vivo* insulin secretion in rats. Diabetes 1994; 43: 1173–9.

Brownlee M. The pathobiology of diabetic complications: a unifying mechanism. Diabetes 2005; 54: 1615–25.

Buse MG. Hexosamines, insulin resistance, and the complications of diabetes: current status. Am J Physiol Endocrinol Metab 2006; 290: E1–8.

Feldman EL, Nave KA, Jensen TS, Bennett DLH. New horizons in diabetic neuropathy: mechanisms, bioenergetics, and pain. Neuron 2017; 93: 1296–313.

Goto Y, Hotta N, Shigeta Y, Sakamoto N, Kikkawa R. Effects of an aldose reductase inhibitor, epalrestat, on diabetic neuropathy. Clinical benefit and indication for the drug assessed from the results of a placebo-controlled double-blind study. Biomed Pharmacother 1995; 49: 269–77.

Greene DA, Arezzo JC, Brown MB. Effect of aldose reductase inhibition on nerve conduction and morphometry in diabetic neuropathy. Zenarestat Study Group. Neurology 1999; 53: 580–91.

Grote CW, Morris JK, Ryals JM, Geiger PC, Wright DE. Insulin receptor substrate 2 expression and involvement in neuronal insulin resistance in diabetic neuropathy. Exp Diabetes Res 2011; 2011: 1–12.

Hardivillé S, Hart GW. Nutrient regulation of signaling, transcription, and cell physiology by O-GlcNAcylation. Cell Metab 2014; 20: 208–13.

Hebert LF Jr, Daniels MC, Zhou J, Crook ED, Turner RL, Simmons ST, et al. Overexpression of glutamine: fructose-6-phosphate amidotransferase in transgenic mice leads to insulin resistance. J Clin Invest 1996; 98: 930–6.

Ho EC, Lam KS, Chen YS, Yip JC, Arvindakshan M, Yamagishi S, et al. Aldose reductase-deficient mice are protected from delayed motor nerve conduction velocity, increased c-Jun NH2-terminal kinase activation, depletion of reduced glutathione, increased superoxide accumulation, and DNA damage. Diabetes 2006; 55: 1946–53.

Hotta N, Akanuma Y, Kawamori R, Matsuoka K, Oka Y, Shichiri M, et al. Long-term clinical effects of epalrestat, an aldose reductase inhibitor, on diabetic peripheral neuropathy: the 3-year, multicenter, comparative Aldose Reductase Inhibitor-Diabetes Complications Trial. Diabetes Care 2006; 29: 1538–44.

Junker BH, Klukas C, Schreiber F. VANTED: a system for advanced data analysis and visualization in the context of biological networks. BMC Bioinformatics 2006; 7: 109.

Kaneto H, Xu G, Song KH, Suzuma K, Bonner-Weir S, Sharma A, et al. Activation of the hexosamine pathway leads to deterioration of pancreatic β-cell function through the induction of oxidative stress. J Biol Chem 2001; 276: 31099–104.

Lim JG, Lee JJ, Park SH, Park JH, Kim SJ, Cho HC, et al. Glucagon-like peptide-1 protects NSC-34motor neurons against glucosamine through Epac-mediated glucose uptake enhancement. Neurosci Lett 2010; 479: 13–7.

Lupachyk S, Watcho P, Stavniichuk R, Shevalye H, Obrosova IG. Endoplasmic reticulum stress plays a key role in the pathogenesis of diabetic peripheral neuropathy. Diabetes 2013; 62: 944–52.

Manfredi G, Yang L, Gajewski CD, Mattiazzi M. Measurements of ATP in mammalian cells. Methods 2002; 26: 317–26.

Masson E, Lagarde M, Wiernsperger N, Bawab S. Hyperglycemia and glucosamine-induced mesangial cell cycle arrest and hypertrophy: common or independent mechanisms? IUBMB Life 2006; 58: 381–8.

McClain DA, Paterson AJ, Roos MD, Wei X, Kudlow JE. Glucose and glucosamine regulate growth factor gene expression in vascular smooth muscle cells. Proc Natl Acad Sci U S A 1992; 89: 8150–4.

Mehdy A, Morelle W, Rosnoblet C, Legrand D, Lefebvre T, Duvet S, et al. PUGNAc treatment leads to an unusual accumulation of free oligosaccharides in CHO cells. J Biochem 2012; 151: 439–46.

Moore JA, Miller WP, Dennis MD. Glucosamine induces REDD1 to suppress insulin action in retinal Muller cells. Cell Sinal 2016; 28: 384–90.

Nakamura M, Barber AJ, Antonetti DA, LaNoue KF, Robinson KA, Buse MG, et al. Excessive hexosamines block the neuroprotective effect of insulin and induce apoptosis in retinal neurons. J Biol Chem 2001; 276: 43748–55.

Nishizawa Y, Wada R, Baba M, Takeuchi M, Hanyu-Itabashi C, Yagihashi S. Neuropathy induced by exogenously administered advanced glycation end-products in rats. J Diabetes Invest 2010; 1: 40–9.

Oates PJ. Aldose reductase, still a compelling target for diabetic neuropathy. Curr Drug Targets 2008; 9: 14–36.

O'Brien PD, Hinder LM, Sakowski SA, Feldman EL. ER stress in diabetic peripheral neuropathy: a new therapeutic target. Antioxid Redox Signal 2014; 21: 621–33.

Ohashi Y, Hirayama A, Ishikawa T, Nakamura S, Shimizu K, Ueno Y, et al. Depiction of metabolome changes in histidine-starved *Escherichia coli* by CE-TOFMS. Mol Biosyst 2008; 4: 135–47.

Ooga T, Sato H, Nagashima A, Sasaki K, Tomita M, Soga T, et al. Metabolomic anatomy of an animal model revealing homeostatic imbalances in dyslipidaemia. Mol Biosyst 2011; 7: 1217–23.

Roy Chowdhury SK, Smith DR, Saleh A, Schapansky J, Marquez A, Gomes S, et al. Impaired adenosine monophosphate-activated protein kinase signalling in dorsal root ganglia neurons is linked to mitochondrial dysfunction and peripheral neuropathy in diabetes. Brain 2012; 135: 1751–66.

Saito K, Lee S, Shiuchi T, Toda C, Kamijo M, Inagaki-Ohara K, et al. An enzymatic photometric assay for 2-deoxyglucose uptake in insulin-responsive tissues and 3T3-L1 adipocytes. Anal Biochem 2011; 412: 9–17.

Schindler A, Foley E. Hexokinase 1 blocks apoptotic signals at the mitochondria. Cell Signal 2013; 25: 2685–92.

Semba RD, Huang H, Lutty GA, Van Eyk JE, Hart GW. The role of O-GlcNAc signaling in the pathogenesis of diabetic retinopathy. Proteomics Clin Appl 2014; 8: 218–31.

Sima AA, Bril V, Nathaniel V, McEwen TA, Brown MB, Lattimer SA, et al. Regeneration and repair of myelinated fibers in sural-nerve biopsy specimens from patients with diabetic neuropathy treated with sorbinil. N Engl J Med 1988; 319: 548–55.

Slawson C, Copeland RJ, Hart GW. O-GlcNAc signaling: a metabolic link between diabetes and cancer? Trends Biochem Sci 2010; 35: 547–55.

Soga T, Ohashi Y, Ueno Y, Naraoka H, Tomita M, Nishioka T. Quantitative metabolome analysis using capillary electrophoresis mass spectrometry. J Proteome Res 2003; 2: 488–94.

Sugimoto K, Rashid IB, Shoji M, Suda T, Yasujima M. Early changes in insulin receptor signaling and pain sensation in streptozotocin-induced diabetic neuropathy in rats. J Pain 2008; 9: 237–45.

Sugimoto M, Ikeda S, Niigata K, Tomita M, Sato H, Soga T. MMMDB: mouse multiple tissue metabolome database. Nucleic Acids Res 2012; 40: D809–14.

Tsuboi K, Mizukami H, Inaba W, Baba M, Yagihashi S. The dipeptidyl peptidase IV inhibitor vildagliptin suppresses development of neuropathy in diabetic rodents: effects on peripheral sensory nerve function, structure and molecular changes. J Neurochem 2016; 136: 859–70.

Vinik AI, Nevoret ML, Casellini C, Parson H. Diabetic neuropathy. Endocrinol Metab Clin North Am 2013; 42: 747–87.

Weigert C, Friess U, Brodbeck K, Häring HU, Schleicher ED. Glutamine: fructose-6-phopshate aminotransferase enzyme activity is necessary for the induction of TGF-β1 and fibronectin expression in mesangial cells. Diabetologia 2003; 46: 852–5.

Werstuck GH, Khan MI, Femia G, Kim AJ, Tedesco V, Trigatti B, et al. Glucosamine-induced endoplasmic reticulum dysfunction is associated with accelerated atherosclerosis in a hyperglycemic mouse model. Diabetes 2006; 55: 93–101.

Wieckowski MR, Wojtczak L. Isolation of crude mitochondrial fraction from cells. Methods Mol Biol 2015; 1241: 1–8.

Wu Y-B, Li H-Q, Ren M-S, Li W-T, Lv X-Y, Wang L. CHOP/ORP150 ratio in endoplasmic reticulum stress: a new mechanism for diabetic peripheral neuropathy. Cell Physiol Biochem 2013; 32: 367–79.

Yagihashi S. Glucotoxic mechanisms and related therapeutic approaches. Int Rev Neurobiol 2016; 127: 121–49.

Yagihashi S, Mizukami H, Sugimoto K. Mechanism of diabetic neuropathy: where are we now and where to go? J Diabetes Invest 2011; 2: 18–32.

Yagihashi S, Yamagishi SI, Wada Ri R, Baba M, Hohman TC, Yabe-Nishimura C, et al. Neuropathy in diabetic mice overexpressing human aldose reductase and effects of aldose reductase inhibitor. Brain 2001; 124: 2448–58.

Ziegler D, Papanas N, Vinik AI, Shaw JE. Epidemiology of polyneuropathy in diabetes and prediabetes. Handb Clin Neurol 2014; 126: 3–22.

Zochodne DW. Sensory neurodegeneration in diabetes: beyond glucotoxicity. Int Rev Neurobiol 2016; 127: 151–80.